Available Online: 16 June 2026 DOI: 10.54254/2977-3903/2026.34455

Impacts of sea level rise on tidal dynamics in the Gulf Stream region

Shichen Wei

Tabor Academy, Marion, USA

abbyweishichen07@gmail.com

Abstract. This study investigates how accelerated sea-level rise interacts with tidal dynamics along the East Coast of the United States, which are regions influenced by the Gulf Stream. Using 2004–2019 satellite altimetry, NOAA tide-gauge data, and the Atlantic Meridional Overturning Circulation (AMOC) index, the analysis reveals that both sea-surface height (SSH) and tidal range (TR) exhibit consistent increases. Although their year-to-year variations are weakly linked, SSH and TR share a strong long-term slope change. We speculate that increases in SSH may deepen the water and are associated with increased TR, although the underlying mechanisms remain uncertain. Integrating AMOC reanalysis data indicates that the weakening of its circulation likely drives the SSH rise and tidal changes. A potential regime transition around 2020 introduces new uncertainty, suggesting the AMOC system may be entering a different dynamical state. These findings highlight the need for improved multi-decadal modeling to support coastal resilience and future ocean renewable energy station planning.

Keywords: Gulf Stream variability, tidal amplification, sea-level acceleration, AMOC weakening, coastal hydrodynamics

1. Introduction

In recent years, global warming has led to increased ocean thermal expansion and glacial melting, which in turn have caused the global Mean Sea Level (MSL) to rise at an accelerated rate. Sea Level Rise (SLR) has serious impacts on coastal areas, including erosion and compound flooding. For example, cities such as Norfolk, Virginia, have long faced chronic tidal flooding issues. Additionally, SLR influences sediment dynamics, coastal wetland stability, and tidal behavior [1]. Tidal changes may disrupt fish migration and spawning cycles, causing economic losses for marine-dependent communities. At the same time, tidal renewable energy is sensitive to changes in water depth. SLR may shift tidal range hotspots or reduce turbine efficiency, adding uncertainty to future tidal energy site selection [2]. Consequently, analyzing past tidal behavior is essential for improving coastal protection and identifying suitable locations for tidal power generation.

The Gulf Stream is a strong western boundary current that brings warm water from the Gulf of America into the Atlantic Ocean. As part of the North Atlantic Gyre, it influences climate along the eastern United States and western Europe. Meanwhile, rising sea levels are rapidly altering global coastlines. For example,

global sea level has risen 8–9 inches since 1880, and projections suggest a rise of up to 2.2 meters by 2100 [3]. More specifically, the MSL acceleration along the U.S. Southeast and Gulf coasts has exceeded 10 mm per year since 2010, increasing faster than in the past 120 years [4]. Haigh et al. (2020) found that in some specific regions, tidal water level changes can approach the magnitude of SLR, with tidal ranges increasing by more than 25 centimeters. SLR deepens coastal waters, reduces bed friction, and may contribute to tidal amplification, although resonance effects may offset these increases depending on location [1]. Although additional modeling suggests uncertainty in future projections, AMOC weakening may contribute more than 10–20 centimeters of additional regional sea level rise, influencing tidal propagation patterns [5-7].

Previous modeling work illustrates this spatial complexity. Pickering et al. (2017) simulated tidal responses under different SLR scenarios and found that MSL increases of 0.5–10 meters may either amplify or weaken tides depending on local conditions [2]. Ross et al. (2017) similarly demonstrated that SLR amplifies high tides in Delaware Bay, while Chesapeake Bay exhibits more complex behavior [7]. Although Pickering et al. (2012) highlighted significant tidal impacts from SLR, Ward et al. (2012) concluded that these changes are often localized and within centimeter-scale magnitudes [8, 9]. Pelling & Green (2019) further showed that the presence or absence of flood protection structures can alter the nonlinear response of tides to SLR [10].

Although many studies have examined the relationship between Sea-Level Rise (SLR) and tidal dynamics, there is still no consensus on the underlying mechanisms. Few studies provide long-term analyses of how SLR and tidal changes interact along the U.S. East Coast, particularly in areas influenced by the Gulf Stream. Additionally, current research rarely integrates measured tidal data with changes in the Gulf Stream (AMOC), limiting the accuracy of future risk modeling and coastal adaptation policy development. This research project aims to investigate the relationship between Sea Level Rise (SLR) and tidal dynamics in the Gulf Stream region of the U.S. East Coast from 2004 to 2019. We hypothesize that the rapid SLR along the East Coast of the U.S. is closely linked to the sustained weakening of the Gulf Stream. This weakening may influence regional tidal dynamics, potentially by increasing water depth and enhancing tidal range.

2. Data and materials

2.1. Research area

This research focuses on the U.S. East Coast region. This area is identified as a hotspot for increased sea level rise, which can amplify storm surge, exacerbate hurricane-driven flooding, and increase overall coastal flood risk along the eastern seaboard. According to Ezer et al. (2013), the sea level in this region is sensitive to fluctuations in the strength and position of the Gulf Stream [11]. More specifically, the large estuaries located in the region, such as the Delaware and Chesapeake Bays, are particularly vulnerable to alterations in tidal dynamics [12]. Therefore, it serves as an ideal research area to investigate the coupling mechanisms between regional sea level rise and tidal behavior.

A persistent, long-term increase in mean sea level observed in the Gulf of America provides a new baseline for all coastal processes. Satellite altimetry data for the broader Gulf of America region indicate an increasing trend of 5.1±0.4 mm/year after the removal of seasonal signals (Figure 1b). This rate of rise, which exceeds the global average 3.0±0.4 mm/year (Figure 1a), is hypothesized to alter tidal dynamics in the shallow waters of the continental shelf and within the region’s estuaries.

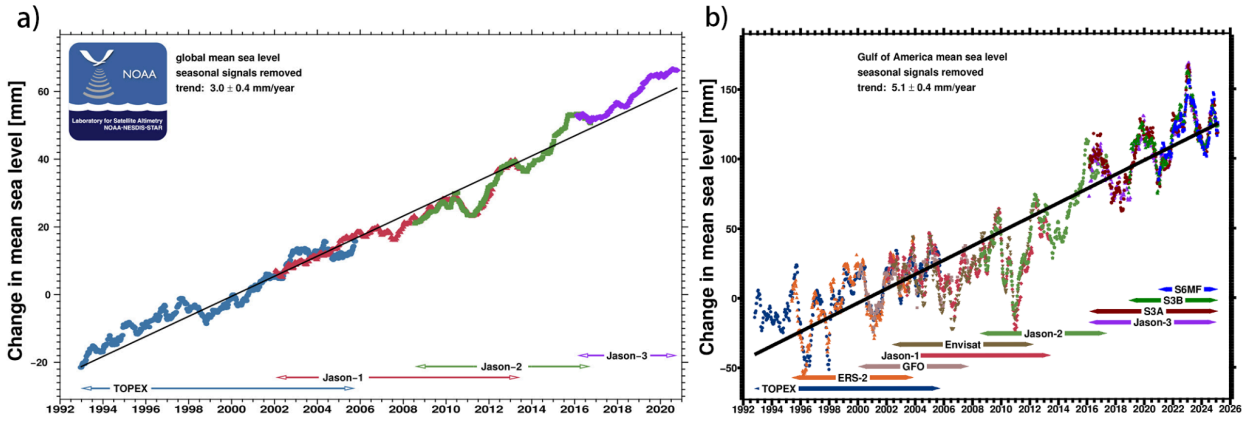

Figure 1. Linear trends in Mean Sea Level (MSL) derived from satellite altimetry over 1993 - 2025 (a) Global mean sea level changes, with seasonal signals removed for 1993-2020. The black line represents a linear trend of 3.0 ± 0.4 mm/yr. (b) Regional mean sea level trend for the Gulf of America (1993-2025), after seasonal corrections. The fitted linear trend (black line) indicates an accelerated rise of 5.1± 0.4 mm/yr. This figure is obtained from multi-mission satellite altimetry (TOPEX, Jason-1, Jason-2, and Jason-3) provided by NOAA (2020) and NOAA/NESDIS/STAR (2025)

This study, accordingly, will analyze the interaction between observed sea level trend and the modulation of key tidal change, particularly the principal lunar semi-diurnal (M2) tide, which dominates the tidal dynamics in this area. This study predicts that SLR in the Gulf Stream region has a direct proportional relationship with tidal range change.

2.2. Data sources and processing

This study uses two primary datasets for analysis and modeling, and was defined to 2004-2019, as this period experienced a significant acceleration in SLR.

The SSH data were obtained from the NASA Jet Propulsion Laboratory's (JPL) Sea Surface Height Anomalies dataset, Version 1 [13]. For this study, the data were spatially constrained to the Gulf Stream region, defined by the coordinates 80°W–60°W longitude and 30°N–45°N latitude. Annual mean SSH anomalies were computed by first averaging the gridded data spatially across all cells within the domain, then averaging these values to produce a single mean value for each year.

Second, the TR data were derived from verified water level records from the tide stations along the U.S [14]. East Coast. A total of 18 NOAA tide gauge stations were selected for this analysis based on the completeness of their records during the 2004–2019 study period. The specific stations used are detailed in Table 1. Annual mean tidal range values were calculated for each individual NOAA tide station separately. For larger regional analyses, these annual values were then averaged across all selected stations to generate a "all-station coupled" mean data for each year.

Table 1. Overview of NOAA tide gauge stations utilize

Station ID	Station Name
8724580	Key West, FL
8723214	Virginia Key (Miami), FL

Table 1. Continued

8721604	Trident Pier, Port Canaveral, FL
8720030	Fernandina Beach, FL
8670870	Fort Pulaski, GA
8665530	Charleston, SC
8658120	Wilmington, NC
8651370	Duck, NC
8638610	Sewells Point, VA
8534720	Atlantic City, NJ
8536110	Cape May, NJ
8518750	The Battery, NY
8510560	Montauk, NY
8452660	Newport, RI
8447930	Woods Hole, MA
8443970	Boston, MA
8418150	Portland, ME
8413320	Bar Harbor, ME

2.3. Methods and equations

To demonstrate the relationship between Sea Surface Height (SSH) and TR, this study employs a set of statistical models. First, the annual SSH and TR variation trend was analyzed using a linear trend model based on Ordinary Least Squares (OLS) regression, where the slope represents the average rate of change in centimeters per year. The OLS estimator of the slope can be determined through equation 1.

$$\beta = \frac{\Sigma_t(t-\underline{t})(y_t-\underline{y})}{\Sigma_t(t-\underline{t})^2} \tag{1}$$

Where t is time, $\bar{t}$ is the mean of all time points, y_t the observed value at time t, and bars indicate sample means.

For the gridded SSH dataset, a pixel-based model was applied in which the slope was computed at each grid cell and aggregated into a regional mean trend through latitude-weighted averaging. The regional slope can be determined through equation 2.

$$\beta = \frac{\Sigma\beta_{pix}cos(\phi)}{\Sigma cos(\phi)} \tag{2}$$

Where β_{pix} is the slope at each grid cell, and ϕ represents latitude.

An anomaly detection model was employed to isolate interannual departures from expected trends. Annual changes were computed as year-to-year differences and baseline slopes were subtracted to yield relative anomalies through equation 3.

$$A_t = (x_t - x_{t-1}) - \beta_{baseline} \tag{3}$$

Where x_t represents the value at year t.

The standardization model was introduced to eliminate the differ in units and variance in SSH and TR datasets. It converts each time series to Z-scores, which processes the data through equation 4.

$$z = \frac{x-\mu}{\sigma} \tag{4}$$

Where μ is the mean and σ the standard deviation. This allowed SSH and TR to be directly compared within the same framework.

Finally, the statistical association between SSH and TR was examined using correlation and regression models. Pearson's correlation coefficient r was used to measure how strongly SSH and TR vary together, with values closer to 1 indicating a stronger positive link. In addition, a simple linear regression was applied to describe how changes in SSH are associated with changes in TR, and can be determined through equation 5.

$$TR \approx a \cdot SSH + b \tag{5}$$

Where the slope describes the empirical association between TR and SSH in the fitted annual regression, and the intercept represents the fitted baseline value when SSH equals zero.

3 Results and discussion

3.1. Trends in sea surface height and tidal range

Since the 1990s, coastal regions influenced by Gulf Stream have experienced a faster rate of Sea Surface Height (SSH) rise than the global average since the 1990s (Figure. 1). To examine whether this increase in SSH also affect tidal behavior, we combined two annual datasets ranged between 2004 to 2019: (i) regional Sea Surface Height (SSH) from PO.DAAC gridded altimetry and (ii) Tidal Range (TR) from 18 NOAA Tides & Currents gauges. Over this period, both the regional Sea Surface Height (SSH) and the station-averaged Tidal Range (TR) increase steadily each year (Figure. 2).

Specifically, the SSH map shows positive slope anomalies off the Carolinas and the mid-Atlantic western boundary (Figure. 2a). Station TR slope reveals net acceleration at many mid-Atlantic and New England gauges (Figure. 2b). Among the 18 stations, the majority exhibited positive slopes, with 16 stations showing positive slopes and two stations displaying negative slopes. To exclude the interference of king tides on the statistics, we employed two methods: excluding (i) daily maximum water levels exceeding the local NOAA mild high tide flood threshold, or (ii) the 99.5th percentile of forecasted high tides during the 2004–2019 period. Based on NOAA's definitions and thresholds for king tides and high-tide flooding, no king tide events were detected within the study window. Consequently, the TR slope presented here reflects background tidal dynamics rather than the influence of extreme high tides.

The patterns of both variables are consistent with the mechanism that friction decreases as water depth changes, which may contribute to tidal amplification of semidiurnal constituents. However, this mechanism is not directly tested in this study. However, some local gauges also have negative slope, potentially caused by resonant node shifts, bathymetric controls, or inlet geometry, that counteract the friction-reduction effect. Key West, FL, and Bar Harbor, ME demonstrate two contrasting responses of tidal range to sea level rise: The Florida Keys have extensive shoals and low tidal ranges, which experienced an overall flattening or slight decrease in tidal range slope from 2004 to 2019. This occurred because sea level rise expanded the coverage of shoals and wetted surfaces, enhancing shallow-water friction and dissipating tidal energy, thereby exerting a slight suppression on amplitude [2]. On the other hand, the Gulf of Maine–Bay of Fundy system is near semidiurnal (M_2) resonance, and the model shows that increases in mean water depth from relative sea-level rise can move the system closer to resonance and amplify tidal ranges [15-18].

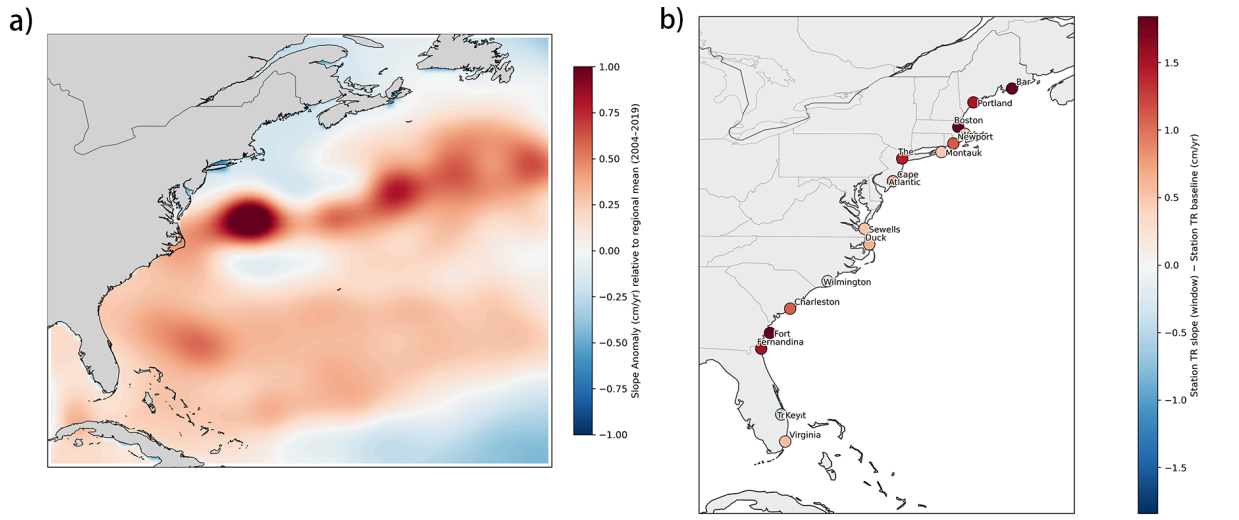

Figure 2. Spatial anomalies of Sea Surface Height (SSH) and Tidal Range (TR) trends along the U.S. East Coast over 2004–2019. (a) Map of pixel-based Sea Surface Height (SSH) slopes relative to the regional mean baseline of 0.65 cm/yr. Red regions indicate areas of above-average sea level rise, while blue regions indicate below-average rise or local decline. (b) Comparison of station-specific TR slopes for 2004-2019 against each station's self 1995-2004 baseline. Red represents acceleration relative to historical conditions, whereas blue shading indicates deceleration

To quantify these trends (Figure. 3), we estimated regional SSH and TR trends separately. The confidence level for all data exceeds C=95%, meaning that there is 95% probability that this "true regression slope" will fall within a positive number. The SSH trend was estimated using a pixel-first approach, in which a linear OLS slope was fit to each altimetry grid cell, and the regional trend was calculated as the cos(latitude)-weighted mean of these per-cell slopes. For TR, we calculate each gauge's annual means and then average across gauges to obtain a station-mean TR series, from which the linear trend was estimated by OLS. Uncertainty intervals were computed with Newey–West (HAC) standard errors to address heteroskedasticity and weak serial correlation. The results rate is 0.770 cm/yr for SSH (n = 16) and 0.402 cm/yr for TR (n = 16). When SSH is plotted on the x-axis and TR on the y-axis, the paired annual values show a strong interannual correlation ($r = 0.806$, $p = 1.65\times10^{-4}$, $n = 16$). An extremely small p-value indicates that the probability of this relationship occurring by chance is virtually zero. Accordingly, we could refer that both variables share a common long-term increasing trend rather than coincidental parallel trends. However, given the limited sample size, these results should be interpreted cautiously as evidence of a strong correlation within the available record rather than a definitive proof.

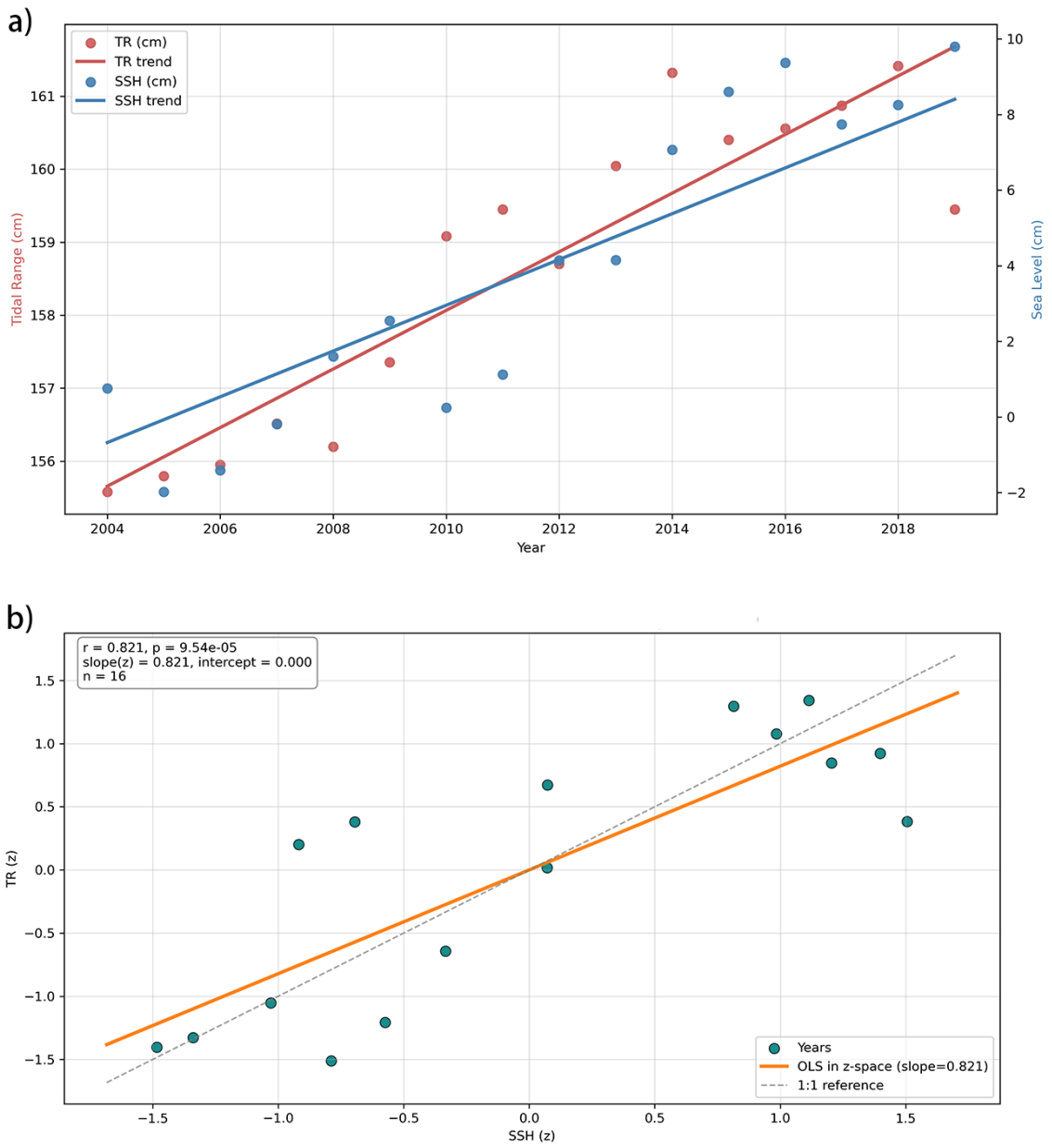

Figure 3. Trends of regional mean Sea Surface Height (SSH) and Tidal Range (TR) along the East Coast of the Gulf Stream region, 2004-2019. (a) Annual regional SSH and station-mean TR time series plotted with points and linear trend lines. The SSH trend is computed with a pixel-first approach. The TR trend is an OLS fit to the annual station-mean TR series .(b) Standardized SSH (z) versus TR (2) for paired years. It includes an OLS regression line (orange) and a 1:1 line reference line

From Figure. 3a, the SSH trend reaches 0.770 cm/yr while the corresponding TR trend estimated from the OLS fit to annual station means is 0.402 cm/yr. The two linear trend line rise nearly in parallel, which reflects a large-scale adjustment across the Gulf Stream over the same period of time. To compare SSH and TR on a dimensionless basis, both variables were standardized using z-scores. The scatter plot of standardized SSH and TR (Figure. 3b) shows a strong positive association ($r = 0.806$, $p = 1.65 \times 10^{-4}$, $n = 16$.) The plot includes both the 1:1 reference line and the fitted OLS regression line in z-space (slope = 0.821). The regression slope lies

close to the 1:1 line, illustrating that years with above-average SSH tend to coincide with above-average TR. Next, a regression of annual TR on SSH (Figure. 4a) shows a slope of 0.431 cm/cm. This slope reflects a shared long-term trend between SSH and TR, indicating that a 1 cm rise is associated with an approximately 0.43 cm increase in TR during 2004-2019. This coherence may reflect that rising SSH shared long-term adjustment with tidal amplification.

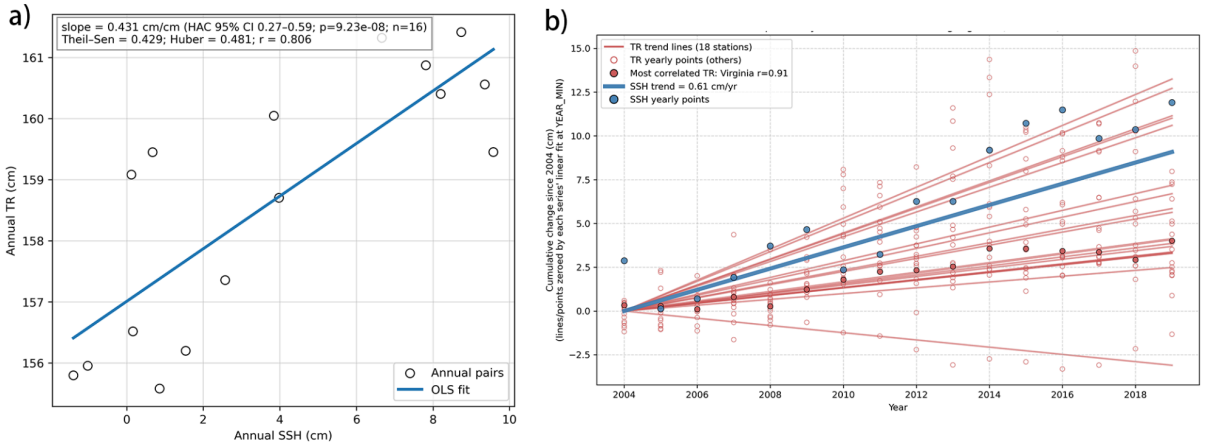

Figure 4. Coupled variability of Sea Surface Height (SSH) and Tidal Range (TR) in the Gulf Stream region over 2004-2019. (a) Linear trend of TR to SSH (cm/cm) from paired annual data. The line shows the OLS fit. Uncertainty intervals are calculated using Newey-West (HAC) standard errors. Estimate slopes using the Theil-Sen and Huber methods. (b) Cumulative SSH and TR trends from 18 tide-gauge stations, with each TR starting from its 2004 baseline. The blue line shows the regional SSH trend (0.61 cm/yr), while red lines represent individual station TR trends, which rise together and show the strongest correlation at Virginia (r = 0.91)

Currently, it appears that years with higher SSH also exhibit larger TR. However, to test whether this reflects a genuine causal linkage or simply a shared long-term trend, we applied two diagnostics: (i) a first-difference regression (ΔTR ~ ΔSSH) and (ii) a year-controlled regression. In the first-difference model, the slope = −0.193 cm/cm and correlation r = −0.326 are insignificant. Similarly, including “year” as a covariate produces an insignificant SSH coefficient β_SSH = −0.133 cm/cm. That is, when we remove the overall upward trend and focus solely on year-to-year fluctuations, the relationship largely disappears. This demonstrates that although the overall model explains substantial variance (R^2 = 0.827), these results suggest the strong correlation shown in Figure. 4a primarily reflects 1 shared long-term rise rather than a direct causal response of TR to SLR.

Cross-correlation analysis further supports this interpretation, where correlation remains high at ±1-year lag (SSH leading TR: r = 0.782; TR leading SSH: r = 0.911). This indicates persistence and a shared slow-acting driving mechanism, rather than an immediate causal sequence. Therefore, the observed slope may reflect a low-frequency, equilibrium adjustment of SSH and TR over the study period. As the mean sea level continues to rise over multiple years, tidal systems gradually "adjust" to a new state of energy equilibrium, resulting in increased tidal range. However, this adjustment may take several years or even decades to fully manifest, and this interpretation remains preliminary. Thus, the 0.43–0.48 cm/cm ratio does not mean "for every 1 cm rise in SSH, TR immediately increases by 0.43 cm the following year." Rather, it signifies that

"against a multi-year background trend, when the overall mean water level rises by 1 cm, the system ultimately achieves a tidal range increase of approximately 0.43 cm."

Collectively, these results indicate that the SSH-TR relationship reflects low-frequency equilibrium rather than instantaneous causality. On a multi-year scale, rising mean sea level deepens continental shelves and estuaries, reducing seabed friction and enabling isostatic tides to increase amplification when geometric conditions permit. However, the specific manifestation of this signal at individual ports remains dependent on site-specific characteristics and influenced by resonance conditions, estuary evolution, and local topography. The spatial variability shown in Figure. 2 reveals the intensity of this equilibrium response.

3.2. Comparison with previous tidal response studies

Devlin et al. (2017) analyzed 152 tide gauges across the Pacific and South China Seas and found that about 35% of stations show significant coupling between the Highest Astronomical Tide (HAT) and Mean Sea Level (MSL), with sensitivities of ±50 mm/m SLR [19]. Their magnitudes of change are lower than our results, likely because they analyzed global sites and used HAT instead of TR. Similar to our finding that SSH and TR exhibit weak year-to-year correlation, Devlin et al. noted that short-term hydrological and meteorological fluctuations often disrupt long-term coupling. Moreover, Haigh et al. (2020) emphasized that the largest tidal amplitude changes occur in shallow estuaries, where not only SLR but also dredging, reclamation, and channel modification strongly affect tidal range [1]. Their findings support the idea that SSH and TR coupling varies with geographic setting and is highly site dependent.

Ross et al. (2017) used hydrodynamic modeling in the Chesapeake and Delaware Bays to show that under no-inundation conditions, SLR increases TR by 10–25% per meter, while the occurrence of adjacent lowlands might cancel out or reverse this amplification [7]. Pickering et al. (2017) further demonstrated in a global modeling framework that fixed-shoreline scenarios generally produce amplification, while inundation or shoreline retreat can reverse the sign of tidal change [2]. This pattern might suggest that our study region remained within a limited-inundation regime. Additionally, Ezer (2019) found that changes in the Gulf Stream and the Atlantic Meridional Overturning Circulation (AMOC) are connected to sea level rise along the U.S. East Coast, suggesting that the change of SSH is the result of the weakening of AMOC [20]. To further test this hypothesis, the following section incorporates AMOC trends into our analysis to examine how the strength of AMOC modulates both Sea-Surface Height (SSH) and TR during 1995-2025

3.3. Influence of AMOC weakening on sea surface height and tidal range dynamics

To explore the connection between ocean circulation and tidal variability, Atlantic Meridional Overturning Circulation (AMOC) time series at 26N from Reanalysis was standardized and compared with SSH and station-mean TR time series [21]. Although these domains are not perfectly located in the same area, AMOC 26° N provides the physically relevant remote driver for the Gulf Stream region. Between 1995 and 2019, the AMOC index demonstrates a persistent negative slope, indicating that the velocity is continuously weakening (Figure. 5a and 5b). The timing of major inflections in AMOC strength corresponds closely to opposite-signed changes in TR and SSH. Therefore, the SSH and TR changes observed over 2004–2019 may reflect shared low-frequency variability linked to large-scale ocean circulation. However, the available data do not allow a definitive attribution of the underlying mechanisms. However, the effects of AMOC on SSH and TR are long-term and gradual, typically exhibiting a multi-year lag that weakens the instantaneous correlation.

Starting around 2020, the correlation between AMOC and SSH/TR starts to weaken. The slope of all three indices shows a simultaneous downturn (Figure. 5a and 5b), leading to a sharp decline in their overall correlation during 1995–2025. Segmented regressions indicate that during 1995–2019, the AMOC–SSH

relationship retains a significant negative slope (-0.72 ± 0.21), while after 2020, the slope becomes weakly positive (+0.18 ± 0.33). This reversal implies a potential regime transition in the coupled system. Physically, rapid stratification and shifts in the Gulf Stream path may have altered resonance and energy propagation on the continental shelf, causing SSH and TR to decline together with ongoing AMOC weakening. However, because the available AMOC index extends only to 2022, the post-2020 behavior cannot be fully discerned. As a result, the short window makes it unavailable to determine whether the change of this pattern would be a continuous decline or another natural cycle of AMOC.

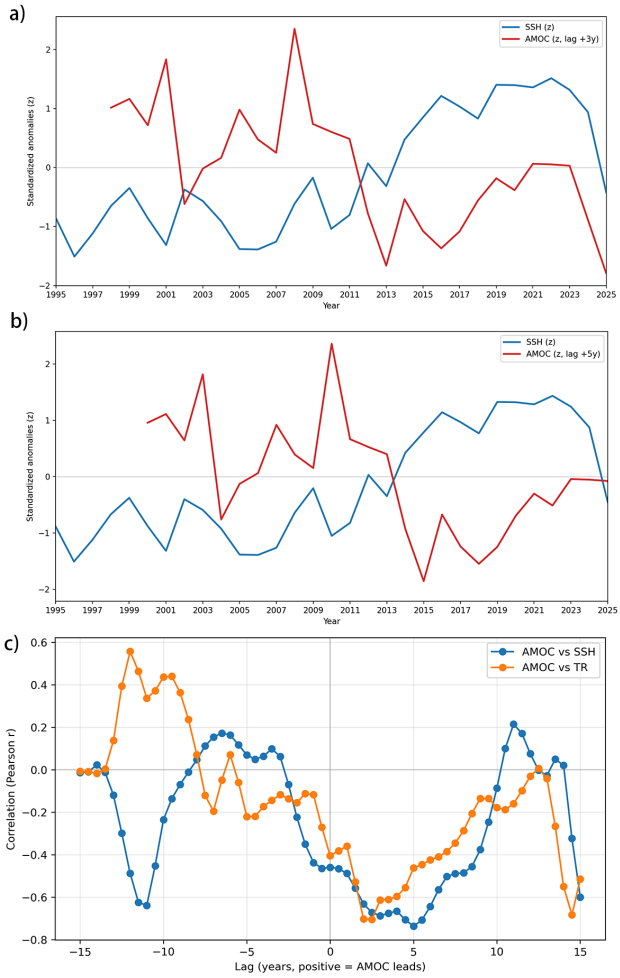

Figure 5. Standardized anomalies (1995 - 2025): AMOC weakening and contrasting trends in Sea-Surface Height (SSH) and Tidal Range (TR) in the Gulf Stream region. All variables were converted to z-scores to eliminate unit differences and allow slope comparison. Linear trends were estimated using Ordinary Least Squares (OLS). (a) The AMOC index (red) shows a negative trend (-0.075 z/yr, $p < 0.001$), while Tidal Range (TR, green) shows a weak positive slope (+0.025 z/yr, $p=0.27$). (b) Similar to 5a, but it is the comparison between the AMOC index (red) and Sea Surface Height (SSH, blue), which shows a positive slope (+0.100 z/yr, $p = 0.27$). (c) Lead–lag correlation between the AMOC index vs SSH and between the AMOC index vs TR, computed at 6-month resolution for lags from –15 to +15 years (positive lags indicate that AMOC leads)

Lead–lag analysis (Figure. 5c) shows that when the AMOC index is shifted forward by approximately three to five years, its correlation with SSH becomes more strongly negative ($r_{+5} \approx -0.75$). When $|r| \approx 0.75$, the two

variables are considered moderately to strongly correlated. Around the lag year, SSH shows a strong negative correlation with AMOC, contrasting with the correlation between TR and SSH, which shows a negative correlation with AMOC at the same temporal offset. Together, these contrasting peaks demonstrate that the SSH and TR responses do not operate on a single uniform timescale but instead reflect multiple adjustment pathways with different physical origins, involving persistence, shared low-frequency variability, or the limited length of the available record rather than a distinct causal sequence. Because AMOC strengthened briefly during 2019–2021, the recent downturn in SSH and TR could represent a delayed reaction to that short-term strengthening. However, we could not exclude the possibility that the change in 2020 is a response to the long-term AMOC weakening. Because the change in 2020 is relatively new from the current time, it remains uncertain whether the post-2020 phase reversal indicates an actual regime shift or a lagged adjustment still in progress. Accordingly, the lead–lag analysis is treated here as an exploratory diagnostic. These complex lag structures help explain why the post-2020 SST, SSH, and TR behavior is difficult to interpret.

4. Conclusion

The results of this study show that sea-level rise and tidal behavior along the U.S. East Coast experienced similar long-term adjustments. The positive trends in both SSH and TR from 2004–2019, together with the strong correlation between their standardized anomalies, indicate that tidal amplification emerged as the coastline adjusted to a rising mean water level. This amplification reflects slow frictional and geometric adjustments rather than short-term causes. When AMOC variability is incorporated, the results suggest that the long-term weakening of AMOC may contribute to the rise of SSH, which may contribute to increases in tidal range, but it represents only one factor within a set of drivers. More specifically, Local air–sea coupling, wind stress, Gulf Stream path shifts, basin geometry, stratification, and estuarine morphology all interact with long-term sea-level changes to shape tidal behavior. At the same time, increased warm and freshwater input caused by climate change could further weaken the AMOC on multi-decadal timescales. It would reduce northward heat transport and alter the spatial pattern of dynamic sea level along the U.S. East Coast. These processes may reshape how SSH anomalies propagate onto the shelf and how tidal systems respond due to the changing conditions. Accordingly, the disruption observed after 2020 in both the SSH, TR, and AMOC indices should not be interpreted as a confirmed regime shift but an exploratory analysis. Still, it is a valuable outlier that may reflect short-term climate fluctuations, an incomplete expression of multi-year lagged AMOC adjustment, or the early stage of a larger circulation reorganization not yet fully expressed in the available data. Nevertheless, because the SSH–TR overlap used in the analysis spans only 16 years, distinguishing these possibilities remains premature and the statistical relationships identified here should be viewed as preliminary and will require validation using longer records and process-based hydrodynamic modeling.

The coupled behavior of SSH and TR has important implications for coastal risk assessment, estuarine hydrodynamics, and future tidal-energy planning. Amplified tidal range may increase the potential for ocean renewable energy but disrupt predictability in some regions. In the meantime, it would also intensify coastal flooding hazards, especially in semi-enclosed bays where higher SSH might occur. Looking ahead, expanding long-term observations of AMOC, SSH, and TR and incorporating higher-frequency circulation proxies, such as Gulf Stream latitude shifts, dynamic sea-level gradients, and wind-driven geostrophic indicators, will be essential for improving data interpretations. More incorporating models that calculate nonlinear feedback, evolving coastal geometry, and multiple external factors will help clarify how SSH, AMOC, and tidal systems evolve under climate change. Ultimately, understanding future coastal hazards will require a multi-factor

framework rather than reliance on any single driver, ensuring more accurate predictions on tidal dynamics and coastal resilience in the Gulf Stream region.

References

[1] Haigh, I. D., Pickering, M. D., Mattias Green, J. A., Arbic, B. K., Arns, A., Dangendorf, S., Hill, D. F., Horsburgh, K., Howard, T., Idier, D., Jay, D. A., Jänicke, L., Lee, S. B., Müller, M., Schindelegger, M., Talke, S. A., Wilmes, B., & Woodworth, P. L. (2020). The tides they are a-changin': a comprehensive review of past and future nonastronomical changes in tides, their driving mechanisms, and future implications. *Reviews of Geophysics, 58*(1), e2018RG000636. https: //doi.org/10.1029/2018RG000636

[2] Pickering, M. D., Horsburgh, K. J., Blundell, J. R., Hirschi, J. J.-M., Nicholls, R. J., Verlaan, M., & Wells, N. C. (2017). The impact of future sea-level rise on global tides. *Continental Shelf Research*, *142*, 50–68. https: //doi.org/10.1016/j.csr.2017.02.004

[3] Global Temperature Anomalies, October 2010. (2010, November 19). NOAA Climate.gov. https: //www.climate.gov/news-features/featured-images/global-temperature-anomalies-october-2010

[4] Dangendorf, S., Hendricks, N., Sun, Q., Klinck, J., Ezer, T., Frederikse, T., Calafat, F. M., Wahl, T., & Törnqvist, T. E. (2023). Acceleration of U.S. Southeast and Gulf coast sea-level rise amplified by internal climate variability. *Nature communications*, *14*(1), 1935. https: //doi.org/10.1038/s41467-023-37649-9

[5] Little, C., Horton, R., Kopp, R. et al. Joint projections of US East Coast sea level and storm surge. *Nature Clim Change 5*, *1114–1120* (2015). https: //doi.org/10.1038/nclimate2801

[6] Gu, Q., Zhang, L., Jia, L. et al. Exploring multiyear-to-decadal North Atlantic sea level predictability and prediction using machine learning. *npj Clim Atmos Sci 7*, *255* (2024). https: //doi.org/10.1038/s41612-024-00802-2

[7] Ross, A. C., Najjar, R. G., Li, M., Lee, S. B., Zhang, F., & Liu, W. (2017). Fingerprints of sea level rise on changing tides in the Chesapeake and Delaware Bays. *Journal of Geophysical Research: Oceans*, *122*(10), 8102-8125. https: //doi.org/10.1002/2017JC012887

[8] M.D. Pickering, N.C. Wells, K.J. Horsburgh, J.A.M. Green, The impact of future sea-level rise on the European Shelf tides, *Continental Shelf Research*, Volume 35, 2012, Pages 1-15, ISSN 0278-4343, https: //doi.org/10.1016/j.csr.2011.11.011.

[9] Ward, Sophie & Green, Mattias & Pelling, Holly. (2012). Tides, sea-level rise and tidal power extraction on the European Shelf. *Ocean Dynamics*. *62.* 10.1007/s10236-012-0552-6.

[10] Holly E. Pelling, J.A. Mattias Green, Impact of flood defences and sea-level rise on the European Shelf tidal regime, *Continental Shelf Research*, Volu*me 85*, 2014, Pages 96-105, ISSN 0278-4343, https: //doi.org/10.1016/j.csr.2014.04.011.

[11] Ezer, T., Atkinson, L. P., Corlett, W. B., & Blanco, J. L. (2013). Gulf Stream's induced sea level rise and variability along the U.S. Mid-Atlantic coast. *Journal of Geophysical Research: Oceans*, *118*(2), 685-697. https: //doi.org/10.1002/jgrc.20091

[12] Lee, S. B., Li, M., & Zhang, F. (2017). Impact of sea level rise on tidal range in Chesapeake and Delaware Bays. *Journal of Geophysical Research: Oceans*, *122*(5), 3917-3938. https: //doi.org/10.1002/2016JC012597

[13] Willis, J. K., Fournier, S., Marlis, K., Killett, E., & Sanchez, J. (2025). NASA-SSH: JPL sea surface height anomalies, Version 1. PO.DAAC, CA, USA. Dataset. Retrieved September 29, 2025, from https: //doi.org/10.5067/NSREF-SG0V1

[14] National Oceanic and Atmospheric Administration, Center for Operational Oceanographic Products and Services. (2025). Water Levels. NOAA Tides & Currents. Dataset. Retrieved September 29, 2025, from https: //tidesandcurrents.noaa.gov/stations.html?type=Water+Levels

[15] GARRETT, C. Tidal resonance in the Bay of Fundy and Gulf of Maine. *Nature 238*, 441–443 (1972). https: //doi.org/10.1038/238441a0

[16] Scott, David & Greenberg, David. (2011). Relative sea-level rise and tidal development in the Bay of Fundy system. *Canadian Journal of Earth Sciences. 20*. 1554-1564. 10.1139/e83-145.

[17] Gehrels, W. R., Belknap, D. F., Pearce, B. R., & Gong, B. (1995). Modeling the contribution of M tidal amplification to the Holocene rise of mean high water in the Gulf of Maine and the Bay of Fundy. *Marine Geology*, *124*(1-4), 71-85.

[18] Greenberg, D. A., Blanchard, W., Smith, B., & Barrow, E. (2012). Climate Change, Mean Sea Level and High Tides in the Bay of Fundy. *Atmosphere-Ocean*, *50*(3), 261–276. https: //doi.org/10.1080/07055900.2012.668670

[19] Devlin, A.T., Jay, D.A., Talke, S.A. et al. Coupling of sea level and tidal range changes, with implications for future water levels. *Sci Rep 7*, *17021* (2017). https: //doi.org/10.1038/s41598-017-17056-z

[20] Ezer, Tal. (2019). Regional Differences in Sea Level Rise Between the Mid-Atlantic Bight and the South Atlantic Bight: Is the Gulf Stream to Blame? *Earth's Future,7,*10.1029/2019EF001174.

[21] Copernicus Marine Service. (2023). Atlantic Meridional Overturning Circulation (AMOC) timeseries at 26° N from reanalysis (Dataset ID: GLOBAL_OMI_NATLANTIC_amoc_max26N_timeseries) [Data set]. https: //doi.org/10.48670/moi-00232